



Cite this: *RSC Adv.*, 2021, 11, 29519

# Synthesis of silver nanoparticles *via* traditional Chinese medicine and evaluation of their antibacterial activities

Yi Yang,<sup>a</sup> Tao Zhao<sup>\*a</sup> and Tao Zhang <sup>\*b</sup>

Silver nanoparticles (AgNPs) are widely used in antibacterial research, but diverse methods for the green synthesis of AgNPs are still underexplored. Phenols, the major components in traditional Chinese medicines (TCMs), can reduce silver ions (Ag<sup>+</sup>) to prepare AgNPs. The representative phenolic compounds are flavonoids and chlorogenic acid (CA) in TCMs. Herein, we report a new strategy to prepare AgNPs *via* decoctions and dregs of TCMs as reductants and dispersants. *Lonicera japonica* flos (LJ), *Astragalus membranaceus* (AM), and *Eucommia ulmoides* bark (EU) were chosen due to their high contents of phenols. <sup>1</sup>H-NMR and HPLC were run to monitor the reaction for AgNP synthesis in decoctions, and XRD and TEM analyses were performed to characterize the synthesized TCMs-AgNPs. In addition, AgNPs prepared by spent Chinese medicinal grounds (SCMGs) were characterized by IR and XRD. The antibacterial assessment demonstrated that these TCMs-AgNPs significantly inhibited the growth of *S. aureus* and *P. aeruginosa* and effectively protected lettuce leaves against *P. aeruginosa* infection. Taken together, this study developed a new synthetic strategy that used decoctions and dregs of TCMs to obtain AgNPs with excellent antibacterial activity, which indicated the potential antibacterial application of these new TCM-based AgNP materials.

Received 20th July 2021  
Accepted 27th August 2021

DOI: 10.1039/d1ra05562c

rsc.li/rsc-advances

## Introduction

Silver at low concentrations exhibits excellent antibacterial activity and is almost nontoxic to human cells.<sup>1</sup> In recent years, as the overuse of antibiotics has caused multiple-drug resistant bacteria, silver's antibacterial properties have been suggested as a possible solution.<sup>2,3</sup> Silver nanoparticles (AgNPs), because of their low price and high antibacterial activity, have been widely applied in daily life. When reacting with water, AgNPs slowly release silver ions (Ag<sup>+</sup>) to penetrate the bacterial membrane and cause dysfunction of enzymes, thus killing the bacteria.<sup>4,5</sup> The general way to synthesize AgNPs is to reduce Ag<sup>+</sup> in silver nitrate (AgNO<sub>3</sub>) to prepare different silver particles in the presence of dispersants. In general, more efficient methods for the green synthesis of AgNPs are still underexplored.

It has been reported that the phenol groups in chlorogenic acid (CA) can reduce Ag<sup>+</sup> and form AgNPs; for example, coffee grains and green tea extracts are good reducing agents to synthesize dispersed AgNPs in aqueous solution.<sup>6–8</sup> CA, as a phenolic compound, is an excellent free radical scavenger and exhibits strong reducing capability.<sup>9–11</sup> *Lonicera japonica* flos (LJ) is a type of traditional Chinese medicine (TCM) widely used in the medicine industry. Modern pharmacological research has

confirmed the high medicinal value of LJ, such as antibacterial,<sup>12,13</sup> antioxidant,<sup>14,15</sup> antiviral<sup>16</sup> and anti-inflammatory effects.<sup>17</sup> *Astragalus membranaceus* (AM) and *Eucommia ulmoides* bark (EU) are also TCMs sufficient in phenols, which can reduce Ag<sup>+</sup> in AgNO<sub>3</sub> to prepare AgNPs. Remarkably, LJ and EU are rich in CA; thus, it is likely that these TCMs can be used as reducing agents to prepare AgNPs.<sup>18–20</sup> Furthermore, TCM waste (dregs) are also considered as excellent reductants, due to the high content of antioxidants on the surface of dregs. Re-using of dregs as reductants in producing virtually useful AgNPs could be economical and eco-friendly.

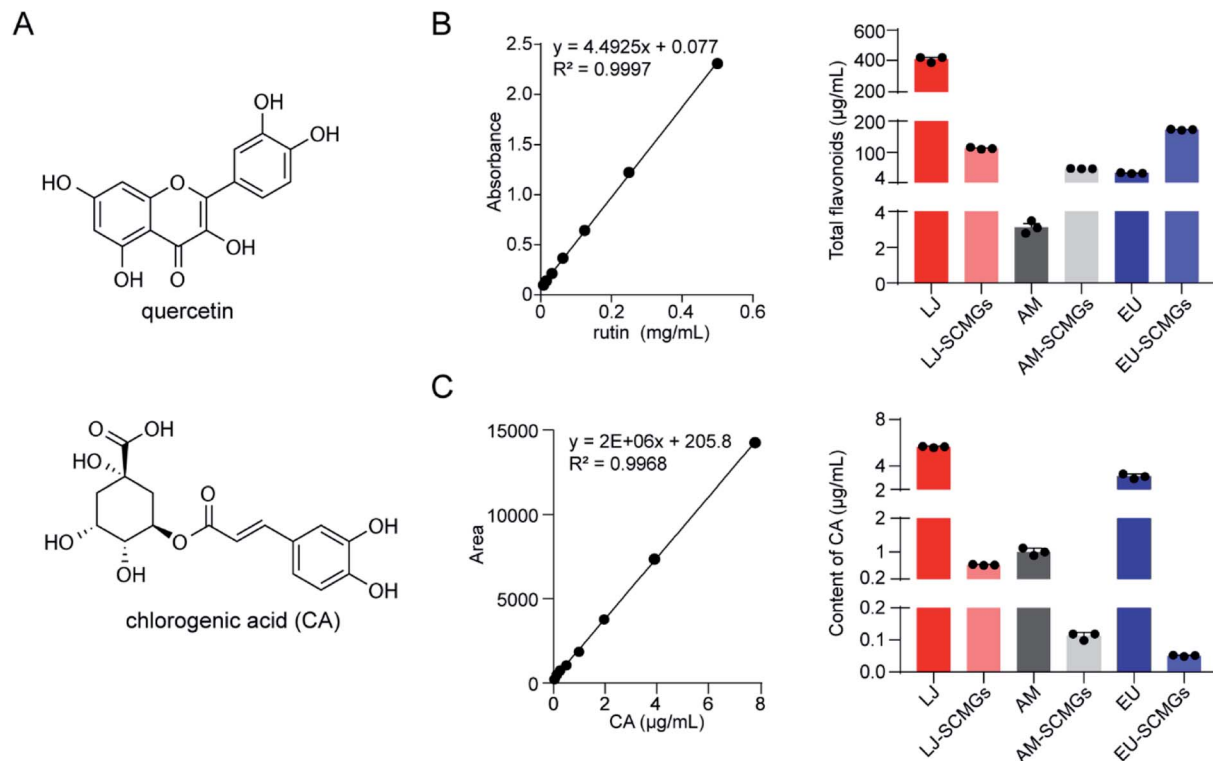
In this work, TCM decoctions were used to synthesize AgNP aqueous solutions (TCMs-AgNPs), and spent Chinese medicine grounds (SCMGs), containing abundant phenolic compounds on the surface, were utilized to synthesize AgNPs as SCMG-supported AgNPs (SCMGs@AgNPs). The obtained nanoparticles were characterized using transmission electron microscopy (TEM), Fourier transform infrared (FT-IR) and X-ray diffraction (XRD). Antibacterial activity tests were conducted in agar plate assays and on lettuce leaves. This study provided a new strategy that used decoctions and dregs of TCMs to simply prepare AgNPs with excellent antibacterial activities.

## Results and discussion

TCMs contain diverse origins of phenolic compounds that significantly contribute to their antioxidant properties and pharmacological activities. As the most abundant components,

<sup>a</sup>Shanghai High School International Division, Shanghai 200231, P. R. China. E-mail: zhaotao@shsid.org

<sup>b</sup>Shanghai Institute of Materia Medica, Chinese Academy of Sciences, Shanghai 201203, P. R. China. E-mail: zhangtao@simm.ac.cn

**Fig. 1** Quantification of reductants in TCMs. (A) Exemplary structures of flavones, for example quercetin and chlorogenic acid (CA). (B) Quantification of total flavonoids in decoction and dregs of LJ, AM and EU, respectively. The calibration curve was prepared by rutin solution, and the linear range was 0.001–0.5 mg mL<sup>-1</sup>. (C) Quantitative detection of CA in decoction and dregs of LJ, AM and EU was performed by LC-MS under positive electrospray ionization (ESI) conditions. The calibration curve was prepared by CA solution, and the linear range was 0.03–7.8 μg mL<sup>-1</sup>.

flavonoids and CA exhibit excellent reducing capacity and can be used as reductants to synthesize AgNPs by reducing silver ions (Fig. 1A). The quantification of flavonoids in the decoctions and dregs of LJ, AM and EU was performed using the AlCl<sub>3</sub> colorimetric method (Fig. 1B). LJ had the highest abundance of total flavonoids (413.4 μg mL<sup>-1</sup>) compared with the decoctions of AM and EU (Table 1). In addition, the dregs of EU-SCMGs were richest in flavonoids (172.2 μg mL<sup>-1</sup>). Meanwhile, the contents of CA in the decoctions and dregs of LJ, AM and EU were quantified by LC-MS analysis (Fig. 1C). Both the LJ decoction and dregs were abounding with CA (Fig. 1C and Table 1). Therefore, as LJ has the most abundant CA content while EU has the richest flavonoid components, the decoction of LJ and EU dregs could be used as reductants in the preparation of AgNPs.

### Strategy for AgNP synthesis by TCMs

Phenolic compounds are considered the dominant reductants in TCMs. However, the usage of these phenolic components in

TCMs as reductants remains largely underexplored. To first determine the viability of synthesizing AgNPs by TCM decoction, we used CA to perform a model reduction reaction to transform silver ions to silver nanoparticles as CA is the most abundant content in TCM decoctions. We proposed that the two phenolic hydroxyl groups of CA could function to reduce Ag<sup>+</sup>, while the hydroxyl groups in quinic acid could be dispersants to stabilize Ag<sup>0</sup>, thus preparing AgNPs (Fig. 2A). <sup>1</sup>H-NMR analysis was performed to trace the preparation of AgNPs through Ag<sup>+</sup> reduction in the presence of CA. The consumption of free CA was monitored by recording the <sup>1</sup>H-NMR spectrum at two time points of 15 min and 24 h (Fig. 2B). After 24 h of incubation, the height of the CA signal peaks decreased dramatically to almost zero compared to the signal peaks corresponding to 15 min of incubation. As the pH of the reaction solution could also affect the reducing capability of CA, therefore, we prepared CA solutions in different pH values with a constant AgNO<sub>3</sub> concentration to investigate the effect of the reaction pH on AgNP synthesis through HPLC analysis (Fig. 2C). When the pH was under 7, the reaction occurred more favourably along with lowering the pH condition, for example, to 3 and 5. If the pH is above 7, the observed decrease in CA abundance declines; meanwhile, the solutions become dark in colour when the pH value further increases, in which Ag<sup>+</sup> is consumed by OH<sup>-</sup> and appears as a black precipitate of AgOH. These data suggested the feasibility of reducing silver ions by phenolic compounds in

**Table 1** Quantification of total flavonoids and CA in the decoction and dregs of TCMs

Content (μg mL <sup>-1</sup> )		LJ	AM	EU
Flavonoids	Decoction	413.4 ± 11.4	3.1 ± 0.2	34.7 ± 0.8
	Dregs	114.9 ± 2.0	48.1 ± 0.3	172.2 ± 0.8
CA	Decoction	5.9 ± 0.04	1.2 ± 0.06	3.0 ± 0.1
	Dregs	0.6 ± 0.008	0.1 ± 0.007	0.1 ± 0.001



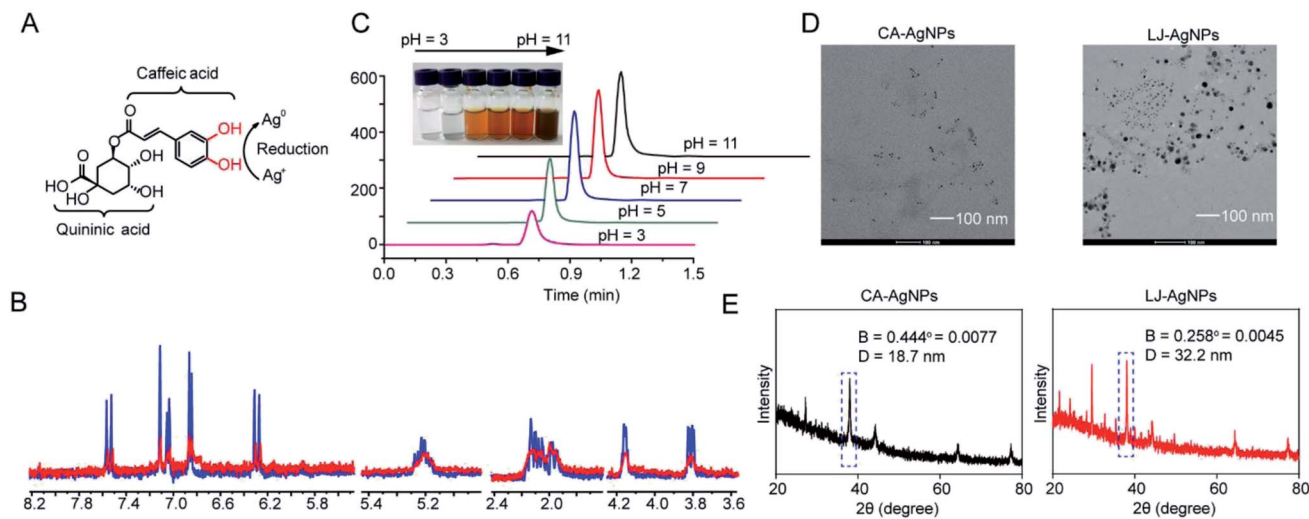


**Fig. 2** Strategy for AgNPs synthesis by TCMs reduction. (A) Two phenolic-hydroxyl groups in caffeic acid could function to reduce  $\text{Ag}^+$ , while the hydroxyl groups in quinic acid could be dispersants to stabilize  $\text{Ag}^0$  in the preparation of AgNPs. (B)  $^1\text{H}$ -NMR records of disappearance of CA signals after 15 min and 24 h incubation with silver nitrate in  $\text{D}_2\text{O}$ . (C) Effect of pH values of CA solution on CA consumption in HPLC analysis, which reflects the formation of AgNPs. (D) Photographs of prepared AgNPs observed by TEM. Left is AgNPs prepared by CA (aq), and right is by LJ decoction, respectively. (E) The sizes of CA-AgNPs and LJ-AgNPs were determined by XRD analysis using Debye-Scherrer method.

TCMs, for example, CA, to prepare nanoparticles under acidic pH conditions.

We subsequently tested whether AgNPs could be prepared by using LJ decoction as a reductant. After simply mixing silver nitrate solution and LJ decoction together at room temperature, TEM was performed to confirm the AgNP formation. TEM images show that AgNPs appear to be irregular particles in shape (Fig. 2D). On the same scale bar, the size of AgNPs that were prepared by LJ decoction was larger than those synthesized from CA (left image in Fig. 2D). It remains underexplored why the sizes are different between the two AgNPs. The sizes of CA-AgNPs and LJ-AgNPs were also determined by XRD analysis using the Debye-Scherrer equation. The diameters are around 18.7 nm and 32.2 nm respectively (Fig. 2E).

### Characterization of AgNPs prepared by TCM decoction

AgNPs are known to exhibit distinct optical properties for surface plasmon resonance (SPR), with a maximum absorption peak at 450 nm. To further investigate the reducing ability of these three decoctions (LJ, AM and EU) for AgNP preparation, TCM decoctions were incubated with  $\text{AgNO}_3$  solution for 12 h, and then, the UV absorbance at 450 nm was measured. The absorbance intensity of AgNPs gradually increased as  $\text{AgNO}_3$  concentration increased before reaching saturation. LJ decoction exhibited the greatest reducing capacity and was saturated at 3.1 mM  $\text{AgNO}_3$  (Fig. 3A). In the same assay, we kept the  $\text{AgNO}_3$  concentration at 3.0 mM and obtained a saturated concentration of CA at 2.5 mM (Fig. 3B). The DPPH radical scavenging activity assay was used to measure the antioxidant activities of these TCM decoctions (Fig. 3C). LJ showed stronger radical scavenging activity than AM and EU due to its high reducing capability, as observed in the quantification of reductants (Table 1). Therefore, we applied LJ decoction as

a reductant because of its high antioxidant ability. We also kept the concentration of  $\text{AgNO}_3$  at 3.0 mM, under which it could be completely reduced by LJ decoction and CA to prepare  $\text{AgNO}_3$ .

### Antibacterial effect of AgNPs prepared by TCM decoction

The antibacterial activities of the LJ-AgNPs and CA-AgNPs were assessed against *S. aureus* Newman using a paper disc diffusion method. The LJ-AgNPs and CA-AgNPs showed antibacterial activity in a concentration-dependent manner (Fig. 3D and E). LJ-AgNPs also exhibited antibacterial activity against the Gram-negative *P. aeruginosa* (PA01) (Fig. 3F). Further assessment of the antibacterial activity of the AgNPs prepared by LJ decoction was performed in the lettuce leaf anti-infection assay, in which PA01 strain was assayed (Fig. 3G). Samples with LJ-AgNPs treatment showed less rotten area caused by *P. aeruginosa* infection compared to the control assays without treatment or with treatment with LJ decoction. These anti-infection assessments indicated that LJ-AgNPs are promising and useful agents in preventing both *S. aureus* and *P. aeruginosa* infections *in vitro*.

### Synthesis of SCMGs@AgNPs

Usually, TCM decoctions are used in clinical treatment, and TCM dregs are largely discarded as medical waste. The traditional extraction method is to boil TCMs with water. However, considerable amounts of flavonoids and CA, which AgNP synthesis requires, remains in the dregs. We considered that these phenolic compounds in dregs could also reduce  $\text{Ag}^+$  to  $\text{Ag}^0$ , thus forming AgNPs on the surface of SCMGs (Fig. 4).

### FT-IR characterization of AgNPs prepared from SCMGs

The functional groups in LJ-SCMGs, LJ-SCMGs@AgNPs, EU-SCMGs and EU-SCMGs@AgNPs were characterized by FT-IR





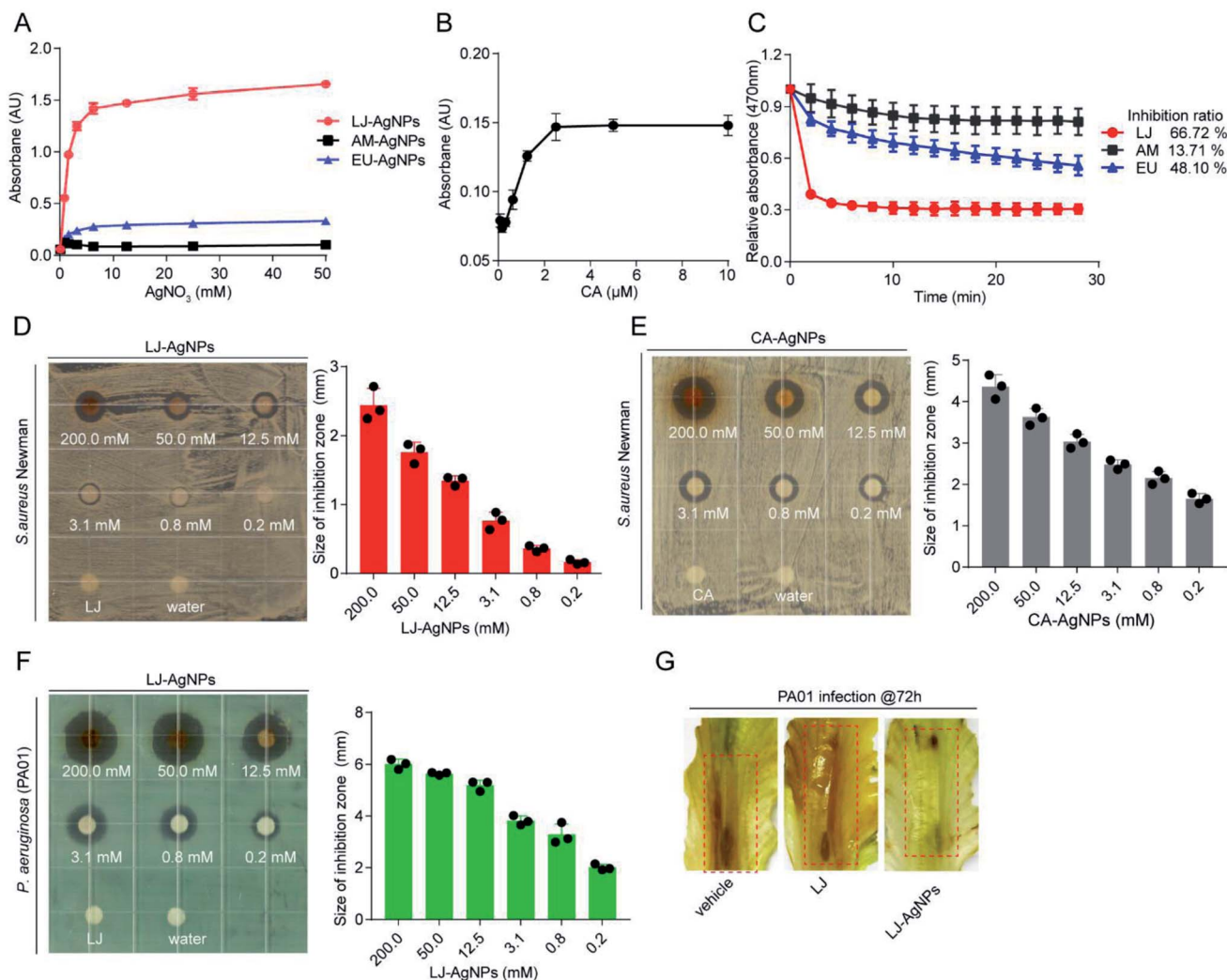


Fig. 3 Characterization of AgNPs preparation and the antibacterial activity. (A) Decoction of LJ, AM and EU reduced Ag<sup>+</sup> to AgNPs in a concentration-dependent manner. (B) CA reduced Ag<sup>+</sup> to AgNPs in a concentration-dependent manner. (C) The DPPH radical scavenging activity of decoctions of LJ, AM and EU. (D) Antibacterial activity of LJ-AgNPs against the strain of *S. aureus* Newman. (E) Antibacterial activity of CA-AgNPs against the *S. aureus* Newman. (F) Antibacterial activity of LJ-AgNPs against the *P. aeruginosa* (PA01). (G) Effect of LJ-AgNPs on *P. aeruginosa* (PA01) infection in lettuce leaves assay. Lettuce leaves were incubated in the presence of PA01 for 72 h with the treatments of vehicle, LJ and LJ-AgNPs, respectively.



Fig. 4 A possible strategy for synthesis of SCMGs@AgNPs by using TCMs drugs.

spectroscopy (Fig. 5A and B). The characteristic peaks of LJ-SCMGs and EU-SCMGs in FT-IR spectrum are almost same. The broad band between 3600 and 3000 cm<sup>-1</sup> is prominent stretching vibrations of -O-H groups in the SCMG spectrum. The two sharp peaks at 2923 and 2852 cm<sup>-1</sup> depend on the

asymmetric stretching of the C-H bonds of the methyl group. Peaks at 1737 cm<sup>-1</sup> are caused by carbonyl vibrations, and an absorption peak at 1647 cm<sup>-1</sup> is the typical stretching vibration of carbonyl vibrations combined with aromatic groups. However, the broad band of stretching vibrations of -O-H groups shifted from 3413 to 2923 cm<sup>-1</sup> (LJ sample) and 3423 to 3388 cm<sup>-1</sup> (EU sample), suggesting that the phenolic groups in LJ-SCMGs and EU-SCMGs participate in the reduction of Ag<sup>+</sup>.

#### Characterization of AgNPs prepared from SCMGs by XRD analysis

To verify the existence of Ag<sup>0</sup> on the surface and in the frame of SCMGs, we performed XRD to analyse AgNP samples supported by LJ-SCMGs and EU-SCMGs (Fig. 5B). In the spectrum of LJ-SCMG@AgNPs sample, there are four unique crystalline peaks at 38°, 44°, 64° and 75°, which indicated the formation of



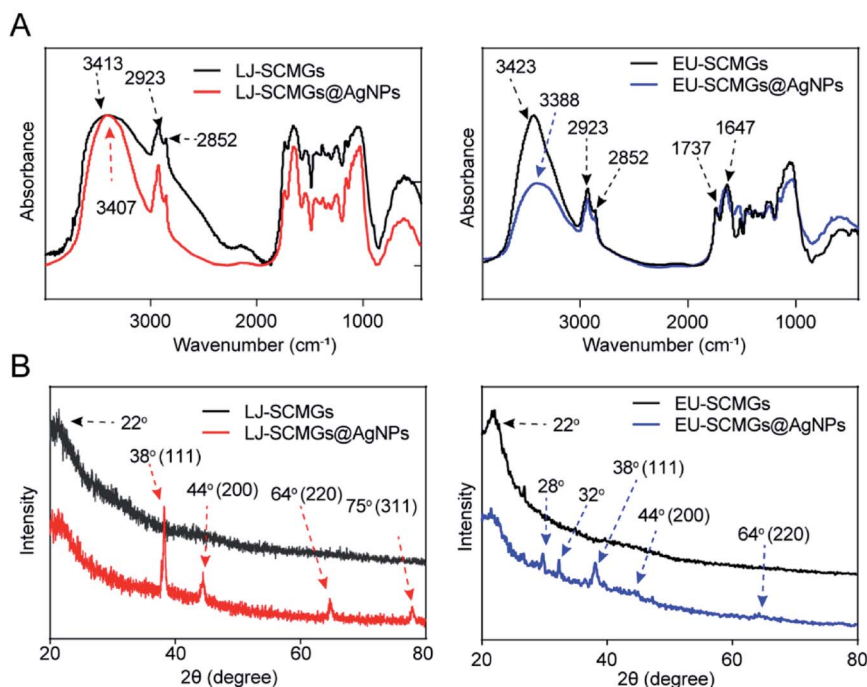


Fig. 5 (A) FT-IR spectra of LJ-SCMGs and LJ-SCMGs@AgNPs (left) and EU-SCMGs and EU-SCMGs@AgNPs (right). (B) XRD patterns of LJ-SCMGs and LJ-SCMGs@AgNPs (left) and EU-SCMGs and EU-SCMGs@AgNPs (right).

AgNPs. In addition, the spectrum of the EU-SCMG sample showed the unique crystalline peak at a  $2\theta$  value of  $22^\circ$  corresponds to cellulose. The XRD patterns of EU-SCMGs@AgNPs show two peaks at  $2\theta = 28^\circ$  and  $32^\circ$ , which indicates the formation of AgCl. The intense peak at  $2\theta = 38^\circ$  and two weak peaks at  $2\theta = 44^\circ$  and  $64^\circ$  indicated the Ag<sup>0</sup> content on the surface of EU-SCMGs@AgNPs based on the silver standard report provided by Joint Committee on Powder Diffraction Standards (JCPDS) file no. 84-0713. In addition to the FT-IR results, XRD analysis also verified the reduction of Ag<sup>+</sup> by SCMGs as a feasible way to synthesize AgNPs.

### Evaluation of the antibacterial activity of TCM-SCMGs@AgNPs

The paper disc diffusion method was used to test the inhibitory activity of SCMGs@AgNPs against the growth of the *S. aureus*

Newman strain. Water and untreated SCMGs were assayed as controls. As shown in Fig. 6A and B, LJ-SCMGs@AgNPs and EU-SCMGs@AgNPs displayed significantly elevated antibacterial effects compared with LJ-SCMGs and EU-SCMGs, and they effectively inhibited bacterial growth in a dose-dependent manner. These results suggested that the discarded dregs of TCMs can function as both reductants and dispersants at the same time in the synthesis of AgNPs for antibacterial agents.

## Experimental

### General methods

All chemicals were analytically pure and used as received. UV absorption was tested on a TECAN SPARK 10M. Agilent 1200 (HPLC) and 6110 (MSD) instruments were utilized to run HPLC traces, obtain mass spectrometry data, and quantify target

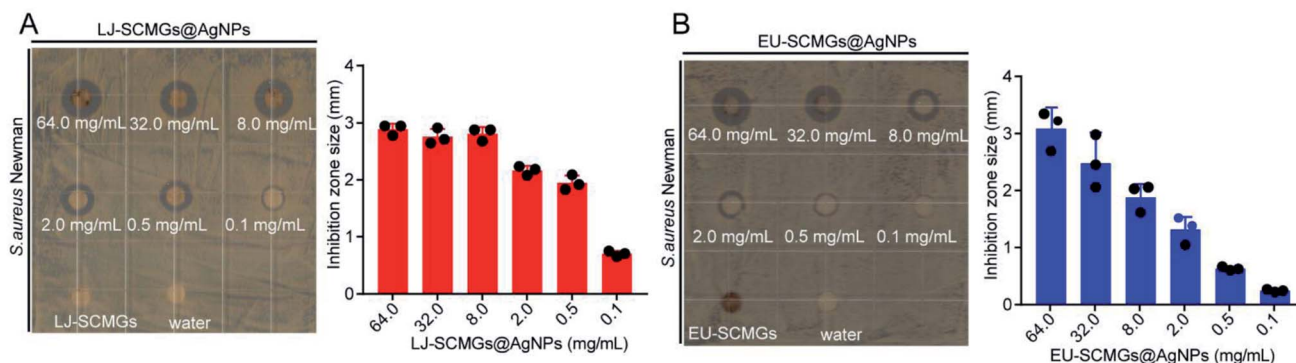


Fig. 6 Antibacterial activity of TCM-SCMGs@AgNPs. (A and B) LJ-SCMGs@AgNPs (A) and EU-SCMGs@AgNPs (B) against the growth of *S. aureus* Newman in a dose dependent manner.

samples. The system was equipped with a PDA UV detector and an Xbridge C18 column (3.5  $\mu\text{m}$ , 4.6  $\times$  50 mm), and separations were achieved at room temperature. The HPLC gradient program utilized 30% to 95% acetonitrile in  $\text{H}_2\text{O}$  in the presence of 0.01% trifluoroacetic acid over 5 min with a 1.5  $\text{mL min}^{-1}$  flow rate.  $^1\text{H}$  NMR spectra were recorded on a Bruker-400 (400 MHz) spectrometer using  $\text{D}_2\text{O}$  as the solvent. A Talos L120C TEM was used to characterize TCM-based AgNPs. A Malvern mastersizer was used to test the particle size distribution. A NICOLET FT-IR 6700 was used to determine functional groups, and an XRD-6000 was used to characterize the AgNP preparation.

### Preparation of the TCM decoctions and spent Chinese medicine grounds (SCMGs)

The dry TCMs (LJ, AM, and EU) were purchased from the Tong Ren Tang pharmacy (Beijing, China), ground with an electric grain mill and sieved through a 30-mesh sieve. TCM powders (2.0 g) were immersed in 100 mL of deionized water. The mixture was held at 80  $^\circ\text{C}$  for 20 min and then cooled to room temperature and filtered. The filtrated decoction was collected and used as a reducing agent. The residue was washed with deionized water, centrifuged three times, soaked in *n*-hexane to degrease three times, and freeze-dried to obtain grains. The grains were ground by mortar and collected as SCMGs.

### Quantification of total flavonoids in TCM decoctions and dregs

Quantification of flavonoids in decoctions and dregs was performed by the  $\text{AlCl}_3$  colorimetric method. The calibration curve was prepared by rutin solutions (linear range: 0.001  $\text{mg mL}^{-1}$  to 0.5  $\text{mg mL}^{-1}$ ). The 200  $\mu\text{L}$  decoction was incubated with 400  $\mu\text{L}$  of  $\text{AlCl}_3$  (aq) in 200  $\mu\text{L}$  of buffer ( $\text{AcONa/AcOH}$ ,  $\text{pH} = 5.2$ ) for 10 min. The dregs soaked in 75% ethanol were placed in an ultrasonic bath for 4 h. After filtration, the filtrate was tested by the  $\text{AlCl}_3$  colorimetric method, and the UV absorbance at 405 nm was recorded. Three technical replicates were taken for each data point, and the data are reported as the mean  $\pm$  SEM.

### Quantification of CA in the decoction and dregs by LC-MS

The quantification of CA in the decoctions and dregs was performed by a LC-MS method under ESI conditions. The calibration curve was prepared by CA solutions (concentrations ranging from 0.03  $\mu\text{g mL}^{-1}$  to 7.8  $\mu\text{g mL}^{-1}$ ). Three technical replicates were taken for each data point, and the data are reported as the mean  $\pm$  SEM.

### Detection of AgNP preparation by UV spectrometry

The saturated concentration of  $\text{AgNO}_3$  that could be completely reduced by decoctions of LJ, AM and EU was tested by UV absorption. The 1 : 1 (v/v) decoction and  $\text{AgNO}_3$  (concentration ranging from 0.1 mM to 50.0 mM) were stirred at room temperature for 12 h. Then, the UV absorbance at 450 nm was recorded by a TECAN SPARK 10M. A similar measurement was applied to the quantification of CA-reducing  $\text{Ag}^+$ . Meanwhile,

1 : 1 (v/v) CA (concentration ranging from 0.1 mM to 10.0 mM) and 6.0 mM  $\text{AgNO}_3$  (aq) were mixed and stirred at room temperature for 12 h. Then, the UV absorbance at 450 nm was recorded by a TECAN SPARK 10M. The data were analysed by using GraphPad Prism software. Three technical replicates were taken for each data point.

### Synthesis of CA-AgNPs

Twenty millilitres of  $\text{AgNO}_3$  (aq) were mixed with 20 mL of 5.0 mM CA (aq) at room temperature. The mixed solution was stirred for 12 h, concentrated and dried to afford CA-AgNPs.

### Synthesis of TCMs-AgNPs by decoction and SCMGs@AgNPs

A 1 : 1 (v/v) solution of 20 mL of 6.0 mM  $\text{AgNO}_3$  (aq) was mixed with 20 mL of the obtained TCM decoction. The mixture was stirred for 12 h at room temperature and then concentrated and dried to produce solid TCMs-AgNPs. For SCMGs@AgNPs, SCMGs (10 mg) were added to 100 mL of 50.0 mM  $\text{AgNO}_3$  solution and stirred for 12 h. After filtration, the residues were washed with deionized water three times and dried at 65  $^\circ\text{C}$  to obtain SCMGs@AgNPs.

### $^1\text{H}$ -NMR analysis of AgNP synthesis

Three hundred microlitres of CA (1.0  $\text{mg mL}^{-1}$ ) and 300  $\mu\text{L}$  of  $\text{AgNO}_3$  (10.0 mM) were mixed in  $\text{D}_2\text{O}$  at room temperature.  $^1\text{H}$ -NMR spectra were recorded at 15 min and 24 h, respectively. The spectra were analysed using MestReNova software.

### HPLC analysis of AgNP synthesis by varying the pH

One hundred millilitres of 1 mM  $\text{AgNO}_3$  was mixed with 10 mL of CA (1  $\text{mg mL}^{-1}$ ), and the solution was stirred at room temperature for 6 h. The solution was then adjusted with 1 M NaOH to pH values of 7, 9, and 11 or with 1 M  $\text{HNO}_3$  to pH values of 3 and 5. The mixture was centrifuged, and the CA content was quantified by HPLC at 254 nm. Three technical replicates were taken for each data point.

### Characterization of TCM-AgNPs by transmission electron microscopy (TEM)

The collected TCM-AgNP sample was stirred at room temperature for dispersion and then placed on a copper grid. The copper grid was dried under an incandescent lamp and then loaded with the sample for TEM. Images were collected at the scale bar of 100 nm.

### Characterization of CA-AgNPs and LJ-AgNPs diameters by X-ray diffraction (XRD) analysis

The process was operated at 40 kV and with a current of 40 mA with  $\text{Cu/K}\alpha$  radiation ( $\lambda = 1.5405 \text{ \AA}$ ) in the range of  $2\theta$  angles of 20–80 $^\circ$  at with a scanning speed of 0.05 $^\circ \text{ s}^{-1}$ . The diameters of CA-AgNPs and LJ-AgNPs were calculated using the Debye-Scherrer equation.

$$D = 0.89\lambda/B \cos \theta$$





Where  $\lambda$  is the wavelength of the X-rays,  $B$  is the width at  $38^\circ$  (full width at half-maximum) of the X-ray diffraction peak in radians,  $\theta$  is the Bragg angle. This method was also performed to characterize AgNPs preparation by TCM dregs.

### Antioxidant activity of TCMs in the DPPH radical scavenging method

The antioxidant activity of decoctions of LJ, AM and EU was measured in terms of the hydrogen donating or radical scavenging ability using the stable radical DPPH. Fifty microlitres of TCM decoction was added to 96-well plates, and 150  $\mu$ L of 2 mM ethanolic aqueous solution of DPPH was added. Absorbance measurements commenced immediately. The decrease in absorbance at 517 nm was determined continuously with data captured at 2 min intervals by a TECAN SPARK 10M for 30 min. Ethanol aqueous solution (50%) was used as a control and for calibration. All measurements were performed in triplicate. The percent inhibition of the DPPH radical by the samples was calculated according to the formula,

$$\% \text{ Inhibition} = [(A_{(0)} - A_{(t)})/A_{(0)}] \times 100$$

where  $A_{(0)}$  is the absorbance of the control at  $t = 0$  min and  $A_{(t)}$  is the absorbance of the antioxidant at 30 min.

### Antibacterial evaluation of AgNPs on the agar plate

The *S. aureus* Newman strain and *P. aeruginosa* PA01 strain were cultured in tryptic soy broth (TSB) overnight, and the OD<sub>600</sub> was adjusted to 0.1. Small pieces of filter paper were soaked in TCMs-AgNPs and SCMGs@AgNPs for 1 h, and the soaked filter paper was placed onto the surface of a Petri dish containing each bacterium. The samples were incubated at 37 °C for 24 h. The inhibitory zone for bacterial growth was observed to evaluate the antibacterial activity

### Fourier transform infrared (FT-IR) analysis

The FT-IR spectrum of the film sample was characterized by using the KBr dispersive method. FT-IR analysis was conducted in the absorbance mode, and the wavenumber range was from 4000 to 500  $\text{cm}^{-1}$  with a resolution of 4  $\text{cm}^{-1}$ .

### Anti-infection of AgNPs in the lettuce leaf assay

The *P. aeruginosa* PA01 strain was grown overnight at 37 °C with shaking (250 rpm) in PB broth. The strain was collected and resuspended, diluted in sterile  $\text{MgSO}_4$  (10.0 mM) and adjusted to an OD<sub>600</sub> of 0.4. Lettuce leaves were prepared by washing with sterile deionized  $\text{H}_2\text{O}$  and 0.1% bleach. Then, the cells were treated with 8  $\mu$ L of *P. aeruginosa* in the absence or presence of 8  $\mu$ L of 10.0 mM LJ-AgNPs as indicated. The inoculated leaves were kept in a growth chamber containing Whatman paper moistened with 10.0 mM  $\text{MgSO}_4$  at 37 °C for 72 h. Symptoms were monitored daily.

## Conclusions

Currently, the overuse of antibiotics has led to bacterial resistance to severe situations. Increasing recognition and understanding of antibiotic resistance has encouraged experts to develop new and more effective antimicrobial agents, and AgNPs could be one of the promising solutions to this issue. Therefore, we utilized TCMs such as LJ, AS and EU decoctions and SCMGs to accomplish synthesis of two types of AgNPs, TCMs-AgNPs and SCMGs@AgNPs. A variety of characterizations were performed to verify the existence of AgNPs and to briefly deduce the mechanism using chlorogenic acid as the model compound. Combined with antibacterial tests on agar plates and lettuce leaves, we verified the capability of both types of synthesized AgNPs to inhibit the growth of both Gram-positive and Gram-negative bacteria *in vitro*. Of note, to the best of our knowledge, this is the first study that utilized dregs, the wasted value of TCMs, to prepare TCM-supported AgNPs, which is economical and eco-friendly. In summary, this study provided a basis for the future usage of TCM-supported AgNPs such as TCMs-AgNPs and SCMGs@AgNPs, which could be promising in the development of new antibacterial agents and materials.

## Abbreviations

AgNPs	Silver nanoparticles
AM	<i>Astragalus membranaceus</i>
CA	Chlorogenic acid
DPPH	2,2-Diphenyl-1-picrylhydrazyl
ESI	Electrospray ionization
EU	<i>Eucommia ulmoides</i> bark
FT-IR	Fourier transform infrared
JCPDS	Joint Committee on Powder Diffraction Standards
LJ	<i>Lonicera japonica</i> flos
SCMGs	Spent Chinese medicine grounds
TCM	Traditional Chinese medicine
TEM	Transmission electron microscope
XRD	X-ray diffraction

## Author contributions

All authors conceived the project. T. Zhang designed the research. Y. Y. performed the experiments and contributed data analyses with help of T. Zhao and T. Zhang. All authors wrote the paper and reviewed the results and approved the manuscript.

## Conflicts of interest

There are no conflicts to declare.

## Acknowledgements

We are grateful to Professor Lefu Lan for supervising the research and experiments.



## Notes and references

- 1 D. P. Tamboli and D. S. Lee, *J. Hazard. Mater.*, 2013, **260**, 878.
- 2 B. Ruttkay-Nedecky, S. Skalickova, M. Kepinska, K. Cihlova, M. Docekalova, M. Stankova, D. Uhlirova, C. Fernandez, J. Sochor, H. Milnerowicz, M. Beklova and R. Kizek, *J. Nanosci. Nanotechnol.*, 2019, **19**, 2762.
- 3 G. R. Rudramurthy, M. K. Swamy, U. R. Sinniah and A. Ghasemzadeh, Nanoparticles: alternatives against drug-resistant pathogenic microbes, *Molecules*, 2016, **21**, 836.
- 4 T. Klaus, R. Joerger, E. Olsson and C. G. Granqvist, *Proc. Natl. Acad. Sci. U. S. A.*, 1999, **96**, 13611.
- 5 H. Long, W. C. Kuang, S. L. Wang, J. X. Zhang, L. H. Huang, Y. Q. Xiong, P. Qing, X. Cai and S. Z. Tan, *J. Nanosci. Nanotechnol.*, 2021, **21**, 5120.
- 6 F. K. Nzekoue, S. Angeloni, L. Navarini, C. Angeloni, M. Freschi, S. Hrelia, L. A. Vitali, G. Sagratini, S. Vittori and G. Caprioli, *Food Res. Int.*, 2020, **133**, 109128.
- 7 H. J. Noh, H. S. Kim, S. H. Jun, Y. H. Kang, S. Cho and Y. Park, *J. Nanosci. Nanotechnol.*, 2013, **13**, 5787.
- 8 S. H. Tsou, S. W. Hu, J. J. Yang, M. Yan and Y. Y. Lin, *Nutrients*, 2019, **11**, 2235.
- 9 N. Liang and D. D. Kitts, *Nutrients*, 2015, **8**, 16.
- 10 Z. Liu, J. Zhao, W. Li, L. Shen, S. Huang, J. Tang, J. Duan, F. Fang, Y. Huang, H. Chang, Z. Chen and R. Zhang, *Sci. Rep.*, 2016, **6**, 19095.
- 11 M. S. Tsang, D. Jiao, B. C. Chan, K. L. Hon, P. C. Leung, C. B. Lau, E. C. Wong, L. Cheng, C. K. Chan, C. W. Lam and C. K. Wong, *Molecules*, 2016, **21**, 519.
- 12 H. K. Müştak, E. Torun, D. Özen, G. Yücel, M. Akan and K. S. Diker, *Br. Poult. Sci.*, 2015, **56**, 299.
- 13 J. Yang, Y. C. Li, X. R. Zhou, X. J. Xu, Q. Y. Fu and C. Z. Liu, *Nat. Prod. Res.*, 2018, **32**, 2238.
- 14 Z. Fan, L. Li, X. Bai, H. Zhang, Q. Liu, H. Zhang, Y. Fu and R. Moyo, *Food Sci. Nutr.*, 2019, **7**, 1786.
- 15 T. Zhang, H. Liu, X. Bai, P. Liu, Y. Yang, J. Huang, L. Zhou and X. Min, *Int. J. Biol. Macromol.*, 2020, **151**, 1058.
- 16 Y. Li, W. Cai, X. Weng, Q. Li, Y. Wang, Y. Chen, W. Zhang, Q. Yang, Y. Guo, X. Zhu and H. Wang, *J. Evidence-Based Complementary Altern. Med.*, 2015, **2015**, 905063.
- 17 M. H. Han, W. S. Lee, A. Nagappan, S. H. Hong, J. H. Jung, C. Park, H. J. Kim, G. Y. Kim, G. Kim, J. M. Jung, C. H. Ryu, S. C. Shin, S. C. Hong and Y. H. Choi, *Phytother. Res.*, 2016, **30**, 1824.
- 18 C. Chaowuttikul, C. Palanuvej and N. Ruangrungrasi, *Pharmacogn. Res.*, 2017, **9**, 128.
- 19 J. Xu, H. Hou, J. Hu and B. Liu, *Sci. Rep.*, 2018, **8**, 6561.
- 20 Z. Tang, S. Zang and X. Zhang, *J. Chromatogr. Sci.*, 2012, **50**, 76.

